



Pressure effects on the slug to churn transition

M.J. Watson, G.F. Hewitt*

Department of Chemical Engineering and Chemical Technology, Imperial College of Science, Technology and Medicine, Prince Consort Road, London SW7 2BY, UK

Received 25 January 1999; received in revised form 25 May 1999

With every best wish to Gad Hetsroni on his 65th birthday

Abstract

Experiments are described on the effect of pressure on the slug/churn flow pattern transition in vertical upwards gas–liquid flow. The experiments were conducted with air–water flow in a 32 mm, 12.6 m long tube and the flow regime transitions were determined using the impedance probe. It was shown that the slug/churn transition was well predicted by the model, though this model slightly over-predicted the effect of pressure. © 1999 Elsevier Science Ltd. All rights reserved.

Keywords: Gas–liquid flow; Flooding; Churn flow; Flow regimes

1. Introduction

One of the most important flow regime transitions in vertical two-phase gas–liquid flow (signalling a gross change in flow behaviour) is that between slug flow (Fig. 1(a)) and churn flow (Fig. 1(b)). A *slug* may be defined as a liquid-continuous region which fills the pipe cross section. The slug may of course, contain a dispersion of bubbles and the void fraction in the slug may be relatively high. Nevertheless, it is a distinctive region and the disappearance of such regions marks the end of slug flow and the beginning of churn flow. The churn flow region itself is one in which the flow is highly disturbed and in which large waves flow up the channel interspersed with regions of falling liquid films (Fig. 1(b)). It is the existence of these flow reversals which distinguishes churn flow from annular flow (Fig. 1(c)), though in both cases there is a continuous gas core in the flow.

* Corresponding author.

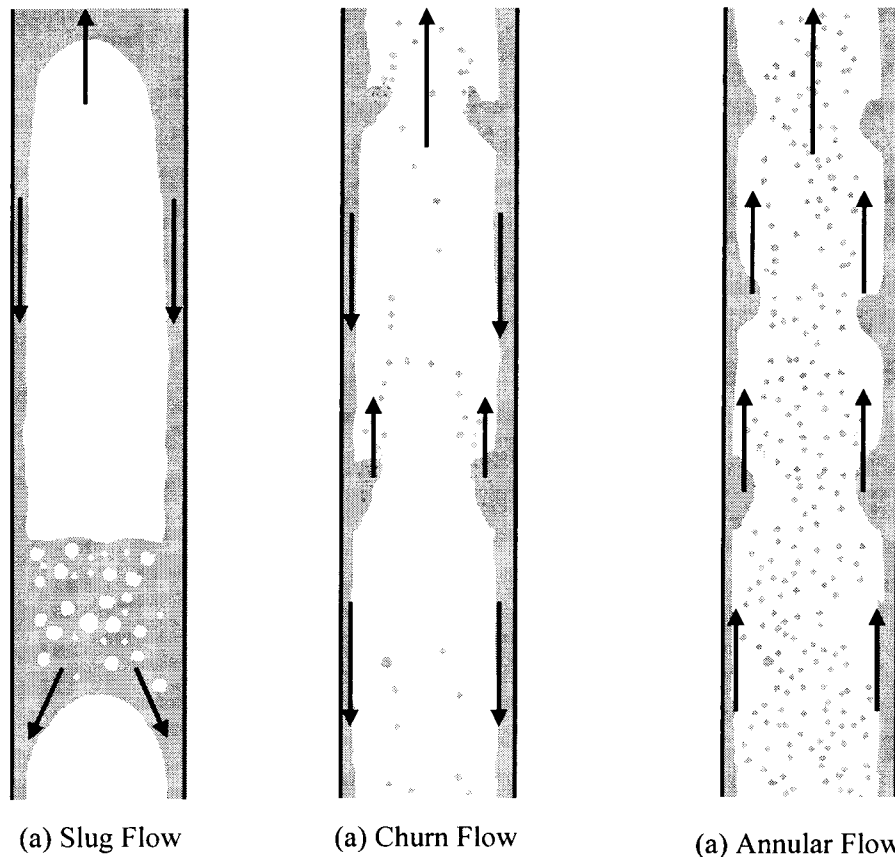


Fig. 1. The slug, churn and annular flow regimes in vertical upwards annular gas-liquid flows.

The objective of the work described in this chapter was to investigate more fully the effect of phase flow rate and pressure on the slug/churn transition and to compare the measurements with a number of competing theories. The experimental method used was to measure the probability distribution of void fraction using an impedance method and to deduce the flow pattern from these measurements. This procedure had also been used by Costigan (Costigan and Whalley, 1997; Costigan, 1997) for experiments at atmospheric pressure and over mass flux ranges $0\text{--}50\text{ kg m}^{-2}\text{ s}^{-1}$ for the gas and $0\text{--}1000\text{ kg m}^{-2}\text{ s}^{-1}$ for the liquid. The present experiments greatly extend the ranges of mass flux and, equally importantly, experiments were carried out over a range of pressure (1.2–5 bar).

In what follows, Section 2 gives a brief description of the competing theories for the slug/churn transition. The new data are presented in Section 3 and comparisons with the various theories are presented in Section 4. The paper closes with a summary of the main conclusions in Section 5.

2. Current slug–churn transition theories

The main approaches to modelling the slug/churn transition have been:

1. Entry region effect. This approach (Taitel et al., 1980) assumes that the churn flow regime is essentially an unstable form of slug flow which occurs only in the entrance region of the pipe. Given sufficient length of pipe, the regime will transform to slug flow until the boundary of annular flow is reached, this boundary corresponding (it was hypothesised) to the gas velocity at which liquid droplets could be suspended in the gas. Though unstable slug flow certainly does exist, it should not be confused with churn flow which is a regime with special characteristics as described above. Thus, this particular interpretation of the transition seems inappropriate. Further discussion of this point is given by Jayanti and Hewitt (1992).
2. Flooding in Taylor bubble region. In this mechanism (first suggested by Nicklin and Davidson, 1962), the transition is initiated by the onset of ‘flooding’ in the liquid film flowing around the Taylor bubble. Flooding is manifested by the onset of upward liquid flow in the countercurrent flow of a falling liquid film and an upward-flowing gas stream. This situation occurs inside the Taylor bubble in slug flow and the slug/churn transition is reached when the fluid velocities are such that flooding occurs. Several authors have proposed this concept; McQuillan and Whalley (1985) developed a theory which embodied the Wallis (1969) correlation for flooding and Jayanti and Hewitt (1992) extended the theory by introducing a new flooding correlation which took account of the length of the falling film. In experiments where the liquid is smoothly injected and removed around the periphery of the tube, and where there is no acceleration of the gas phase at the tube entry, the flooding velocity decreases significantly with the length of the falling film region. Jayanti and Hewitt (1992) argued that a similar effect would occur in the Taylor bubble, thus, the length of the bubble would affect the transition.
3. Excessive aeration of the liquid slug. As flow velocities increase, more and more gas is entrained in the slug; the basis of the excess aeration theories for the slug/churn transition is that, when the void fraction in the slug reaches a critical value, the slug breaks down due to bubble coalescence. The critical condition can be expressed in terms of overall void fraction (Mishima and Ishii, 1984) or in terms of the void fraction in the slug (Brauner and Barnea, 1986). In the latter model, the critical void fraction was taken as 0.52, corresponding to the case of cubic close packing of the bubbles.

The various theories for the transitions give very different results as is illustrated in Fig. 2, where the transitions for a pressure of 5 bar are plotted in terms of U_G and U_L , the gas and liquid superficial velocities.

3. Experimental studies

3.1. Apparatus

The experiments were carried out in the LOTUS (LONg TUBE System) facility at Imperial College. This consists of a 12.6 m long, vertical 32 mm diameter copper tube, in which a wide

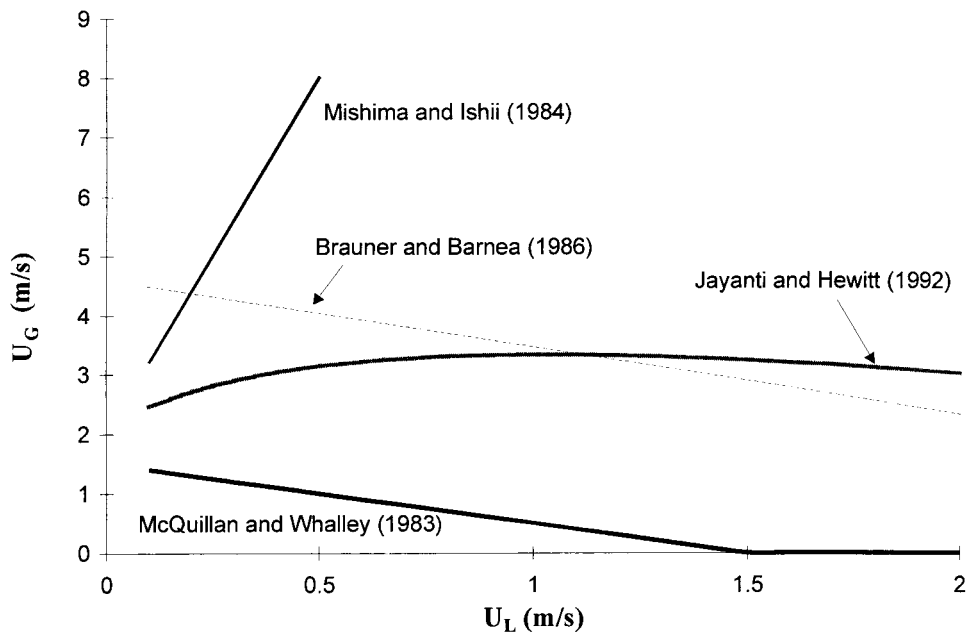


Fig. 2. Comparison of models for the slug/churn transition (air–water flow in a 32 mm bore tube at 5-bar pressure).

range of air and water flowrates can be covered and pressures up to 7 bar can be achieved. To identify the flow patterns, the impedance probe system described by Ma et al. (1991) was used. This probe was also used by Wang et al. (1991) and Costigan and Whalley (1997) for flow pattern identification and provides a non intrusive, simple and cost effective method for high frequency, area averaged, void fraction measurements. On the basis of histograms of the void fraction against time traces produced by the probes, two phase flow regimes can be determined (see Costigan and Whalley, 1997).

Two impedance probes were manufactured locally to fit in the test section of the LOTUS facility. A schematic view of one such probe is shown in Fig. 3.

The probe consists of three layers of two copper ring segments (positive and negative electrode) The rings are and 3.0 mm high (in the axial direction in the tube) and the ends of the ring segments are separated by a gap of 5 mm as shown, mounted flush with the wall in an acrylic section. Each segment spans an arc of 160° . The lower and upper sets of ring segments are grounded to restrict the electric field to the middle segments through which the signal is led. This is to ensure strictly local measurement of the conductance. The water between the input and output segment acts as a conductor and the air as an isolator for the signal. The thin copper strips of the original design are replaced by 3 mm square cross section strips, embedded in the acrylic wall. The part in contact with the flow remains a 3 mm high strip flush with the wall. The probe units are 50 mm high and the ends are machined to fit the LOTUS rig flanges. They can be placed at several distances from each other in the rig for cross correlation purposes. Two signal processing circuits were built, slight changes being made to the original design described in Ma et al. (1991), the resistance to ground at the input was increased to 87Ω , to increase the signal output. The gain, the input frequency and the offset of

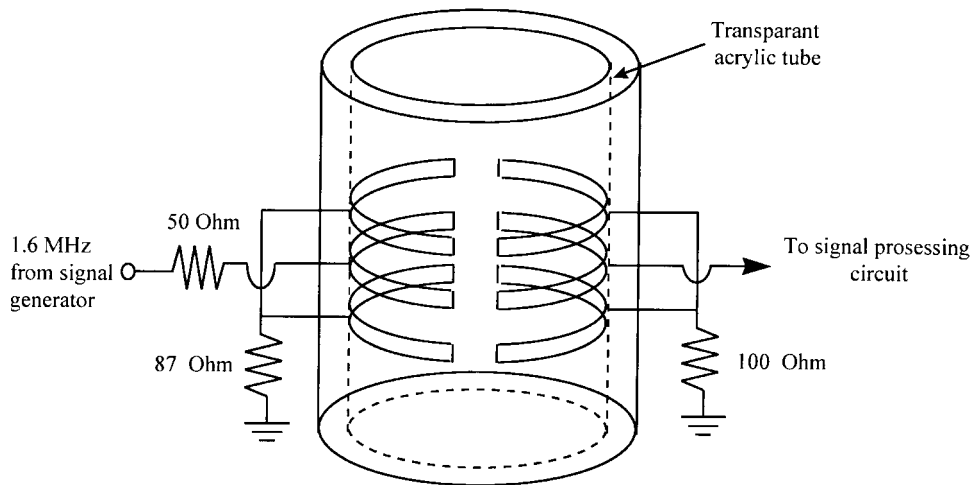


Fig. 3. Diagram of the probe.

the circuits were adjustable via accurate potentiometers, so the probes could be calibrated before each experiment.

The relationship between void fraction and probe output signal is claimed to be linear by Costigan and Whalley (1997) and Ma et al. (1991). This linearity was investigated in the present work by comparing the measurement of time-averaged void fraction with the values obtained, using a traversing gamma densitometer. The comparison is shown in Fig. 4.

Also shown in Fig. 3 are the results from comparing impedance probe measured void fraction to a known annular void fraction. These known void fractions were produced in static, bench scale tests, where annular flow was simulated using different sized concentrically placed plastic rods (the annulus between the rods and the probe elements filled with water from the LOTUS rig). Though the static tests gave results which showed considerable deviation, the dynamic tests on actual flow showed much better linearity, in agreement with the quick-closing valve comparisons of Costigan (1997). This better performance in dynamic testing is probably due to the probe not detecting detached liquid (i.e., droplets) which compensate for the offset. Further details of these comparative studies are given by Watson (1999).

3.2. Range of data

The present experiments were carried out over the flow rate ranges illustrated in Fig. 5. The flowrate ranges were influenced by pressure (as shown) but, even at the highest pressures, the range of flowrates covered was large compared to that encompassed in the study of Costigan and Whalley (1997).

3.3. Experimental procedure

In a typical experiment for the determination of the transition from slug to churn flow, the water flow rate was fixed and measurements were taken at a range of air flow rates in the

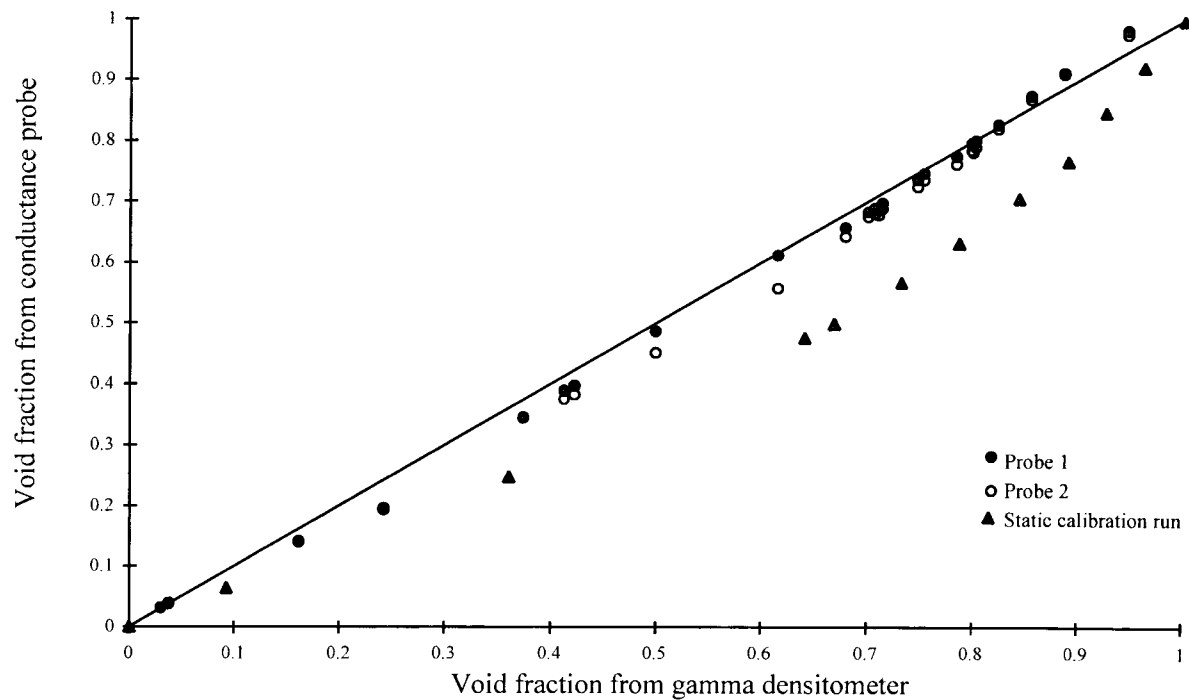


Fig. 4. Comparative experimental data.

vicinity of the transition boundary. At each flow rate, a measurement of the response of the impedance probes was taken every 0.01 s, for 20 s. In slug flow, sample lengths of 20s were

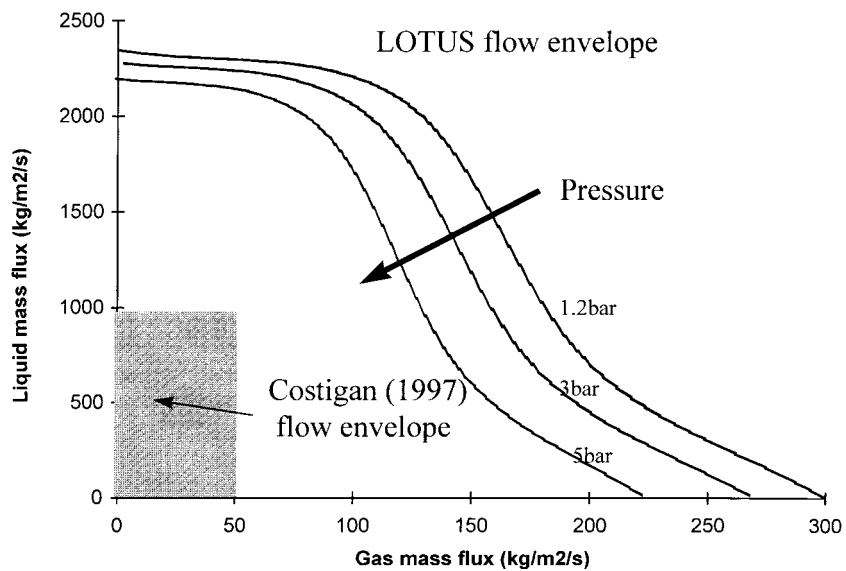


Fig. 5. Flow envelopes.

expected to give a better representation of the flow since the slug frequency can be of the order of 1 Hz at low water flow rates. 100 Hz sampling frequency was chosen as a convenience for the data acquisition program, however, results for higher frequencies (up to 200 Hz) showed no significant difference to those for a 100 Hz sampling frequency. It was therefore assumed that the sampling rate was great enough to record with sufficient clarity all the necessary characteristics of the two flow regimes. During every run the pressure, the differential pressure across the gas orifice plate, temperature, and void fraction traces of the two impedance probes were recorded.

3.4. *Specifying the slug to churn transition*

The slug and churn flow patterns give very different void fraction probability distribution (histograms). Moving from slug to churn, the main differences were: a loss in the low void fraction spike, corresponding to the disappearance of liquid slugs; and an increase in scatter of the high void fraction spike, corresponding to the loss of a stable liquid film.

However, as with all flow pattern transitions, the switch from the slug to the churn regime happens gradually over a range of gas flow rates. The transitional flow pattern may be seen as a mixture of the two regimes, having the occasional stable slug, with less stable, collapsing slugs of less well defined shapes and void fractions. When the gas flow is increased, the peak in the histogram at low flow rate will gradually disappear. This gradual disappearance of the liquid slugs is observable from a series of histograms of experiments at increasing air flow rate (for constant liquid flowrate). An example of a series of histograms is presented in Fig. 6. Some workers define the region of gradual disappearance of the liquid slugs as a separate flow pattern, unstable slug flow (Costigan and Whalley, 1997). However, for the purpose of this investigation, a strict definition of the transition line between slug and churn flow is needed, in order to best observe the effect of pressure on the transition. In order to do this, churn flow was said to exist for a 100 Hz, 20 s trace, if no more than 2 measured void fractions are below 0.37 Fig. 7. Though this criterion is arbitrary, it is based on observations of the disappearance of liquid slugs in the flow, and is a useful benchmark to compare results at different pressures and liquid flowrates. It was found to be independent of measurement frequency and measurement time in the ranges, 100–200 Hz and 10–20 s respectively.

3.5. *Example of transition detection*

Fig. 6 shows a typical set of time traces are with increasing air flow rates. Generally, a set of data to determine the transition at one liquid flowrate, would contain 6–12 such runs, at successively increasing gas velocities, no more than 0.5 m/s apart. From the criterion described in the previous section, the transition is determined to be at run 922, ($U_G = 3.0$ m/s).

3.6. *Results*

The experiments were carried out at pressures (at the measurement section) of 1.2, 3.0 and 5.0 bar. 1.2 bar was the lowest pressure at which a reasonable range of gas and liquid flow rates could be covered. The pressure stated is that of a time average pressure recorded by a

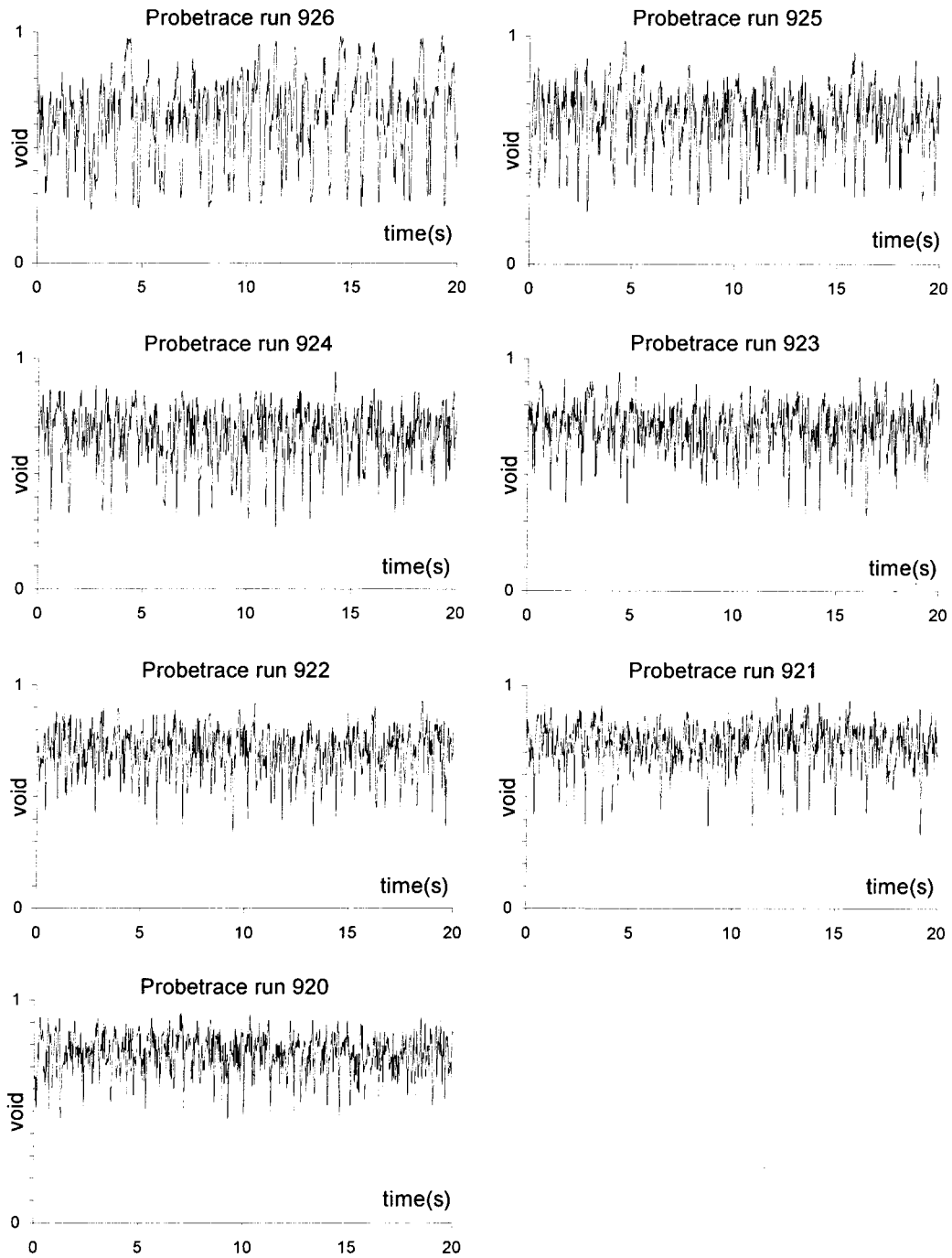


Fig. 6. Probe traces for a liquid superficial velocity (U_L) of 0.84 m s^{-1} with air superficial velocity rising from 1.6 m s^{-1} (run 926) to 3.9 m s^{-1} (run 920) (pressure 1.2 bar).

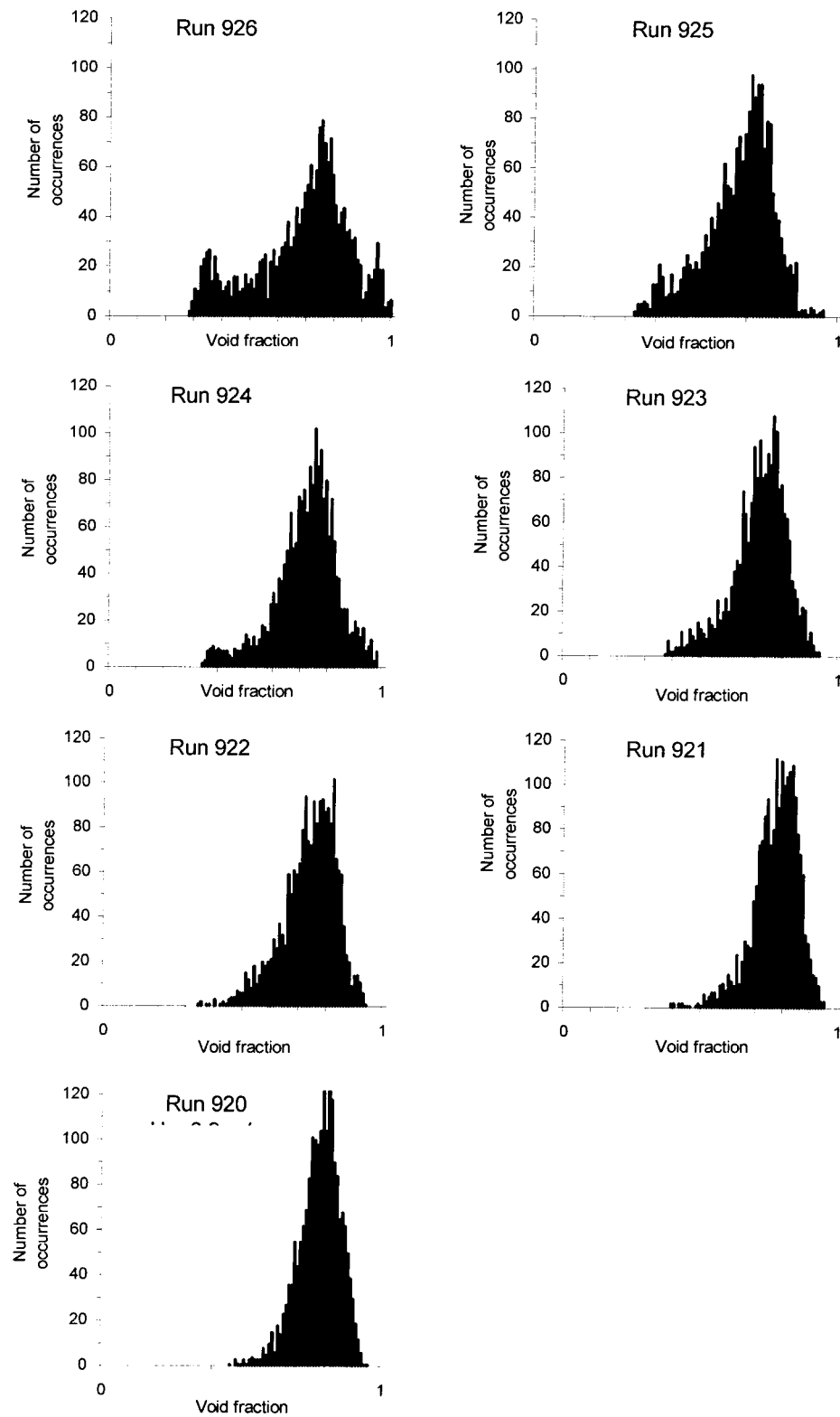


Fig. 7. Void fraction histograms corresponding to the probe traces shown in Fig. 6.

pressure transducer at the measurement section. A 1 s time average was required due to the large pressure fluctuations that are characteristic of the slug and churn flow regimes.

The flow pattern observations are shown in Figs. 8–10 for the respective pressures. For each liquid flow rate for which data was obtained, the transitional gas velocity was determined, and the results for the transition condition are presented in Fig. 11. Table 1 gives the quantitative data. As will be seen from Fig. 11, the transition superficial gas velocity decreases with increasing pressure and increasing superficial liquid velocity.

It is interesting to compare the present data at 1.2 bar with those of Costigan and Whalley (1997) obtained for close to 1 bar pressure and using the same measurement techniques as those applied in the present work. The present data are compared with the Costigan and Whalley (1997) results in Fig. 12. Since Costigan and Whalley were investigating the whole of the flow regime map, it is not surprising that their data are much sparser in the slug–churn transition region, than the data obtained in the present study where the emphasis has been on the transition. However, as will be seen from Fig. 12, the two sets of data are generally consistent. In the Costigan and Whalley 1-bar transition line would be expected to lie slightly above the line representing the present 1.2-bar data.

4. Comparisons with prediction models

The data were compared with the models of McQuillan and Whalley (1985), Jayanti and Hewitt (1992), Mishima and Ishii (1984) and Brauner and Barnea (1986). The results of the

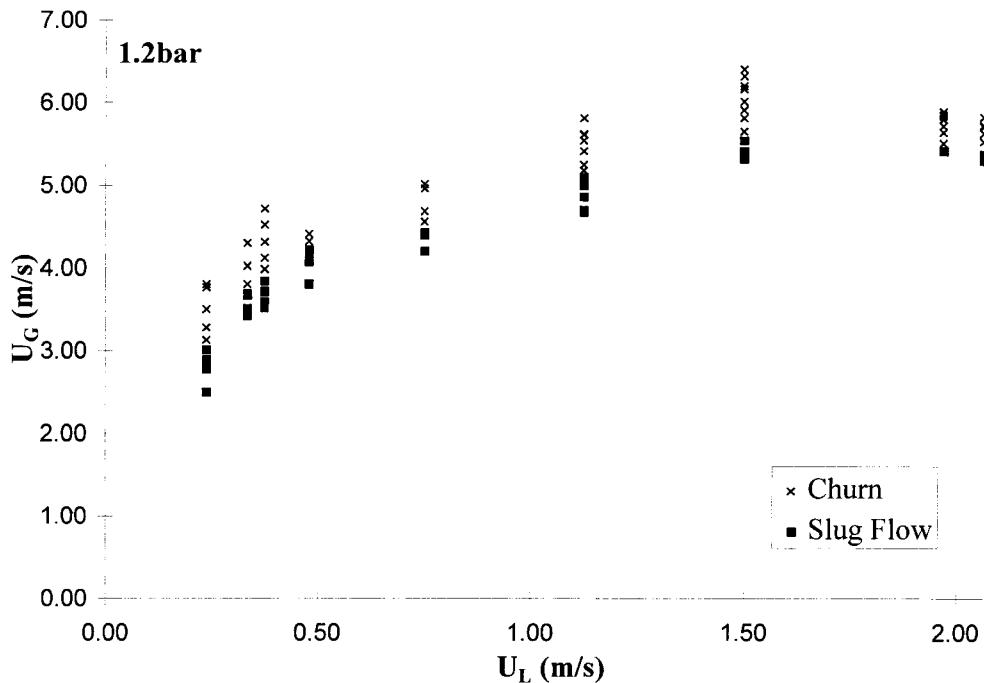


Fig. 8. Flow pattern observations at 1.2-bar pressure.

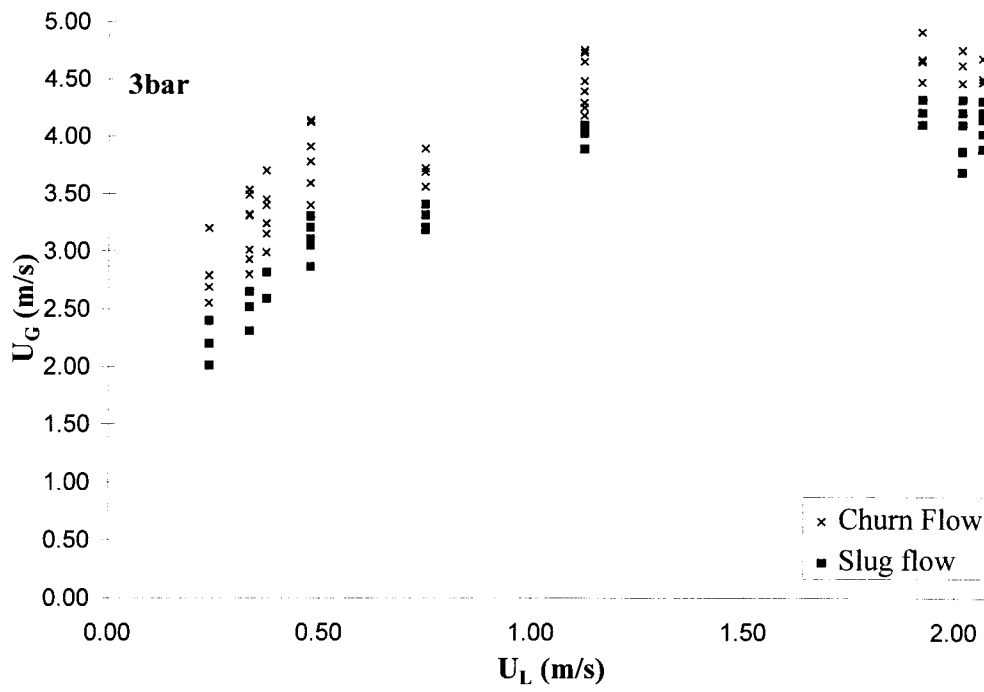


Fig. 9. Flow pattern observations at 3.0-bar pressure.

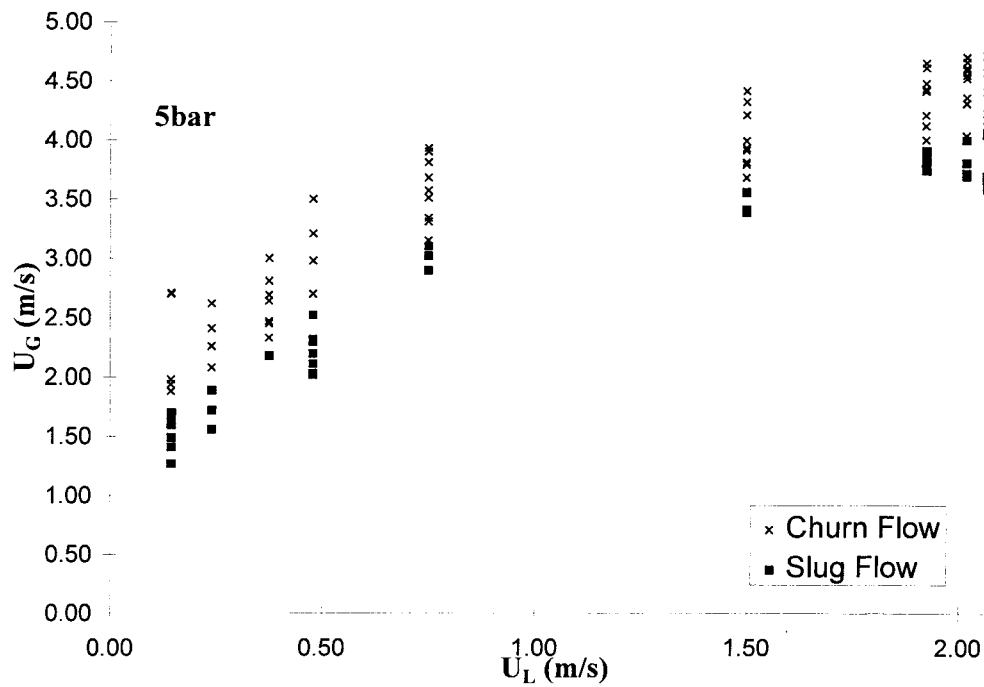


Fig. 10. Flow pattern observations at 5.0-bar pressure.

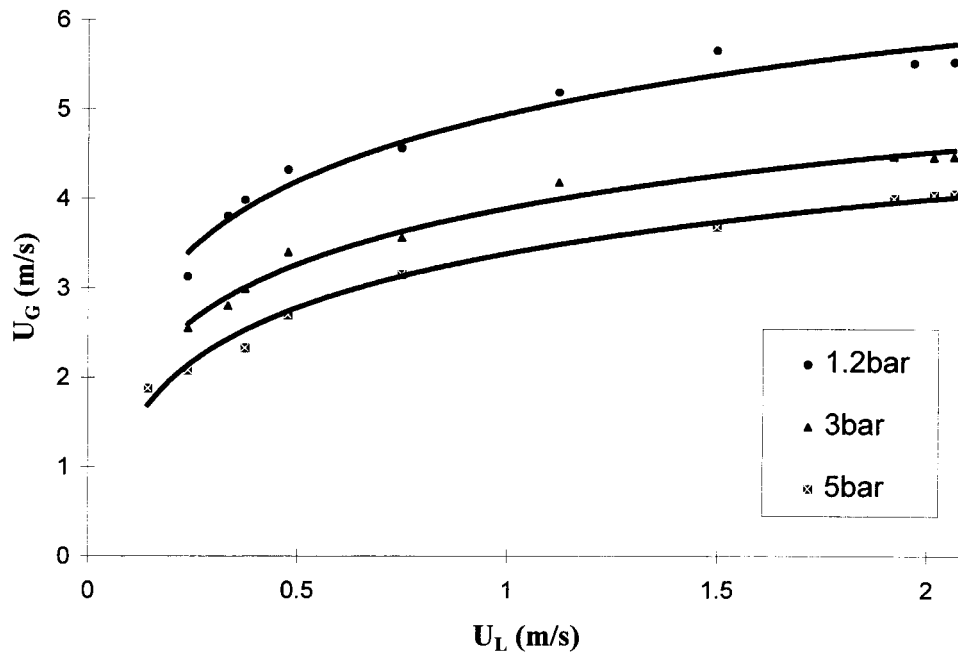


Fig. 11. Slug/churn transition data.

comparisons are shown in Figs. 13–15 for 1.2-, 3.0- and 5.0-bar pressure respectively. The following observations may be made:

1. The model of McQuillan and Whalley predicts the opposite to the observed trend with

Table 1
Experimental transition data

U_L (ms^{-1})	U_G (ms^{-1})		
	1.2 bar	3.0 bar	5.0 bar
0.14	–	–	1.88
0.24	3.13	2.55	2.08
0.33	3.80	2.80	–
0.37	3.98	2.99	2.33
0.48	4.32	3.40	2.70
0.75	4.56	3.56	3.15
1.12	5.18	4.18	–
1.50	5.65	–	3.68
1.92	–	4.47	4.00
1.97	5.51	–	–
2.01	–	4.46	4.04
2.06	5.53	4.47	4.06

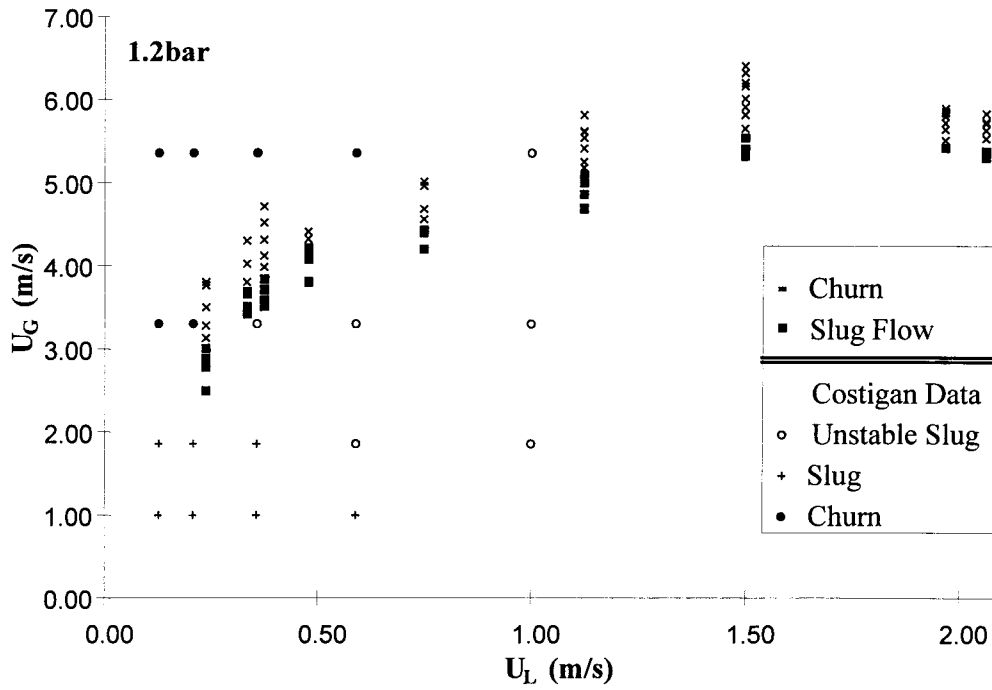


Fig. 12. Comparison with Costigan and Whalley (1997).

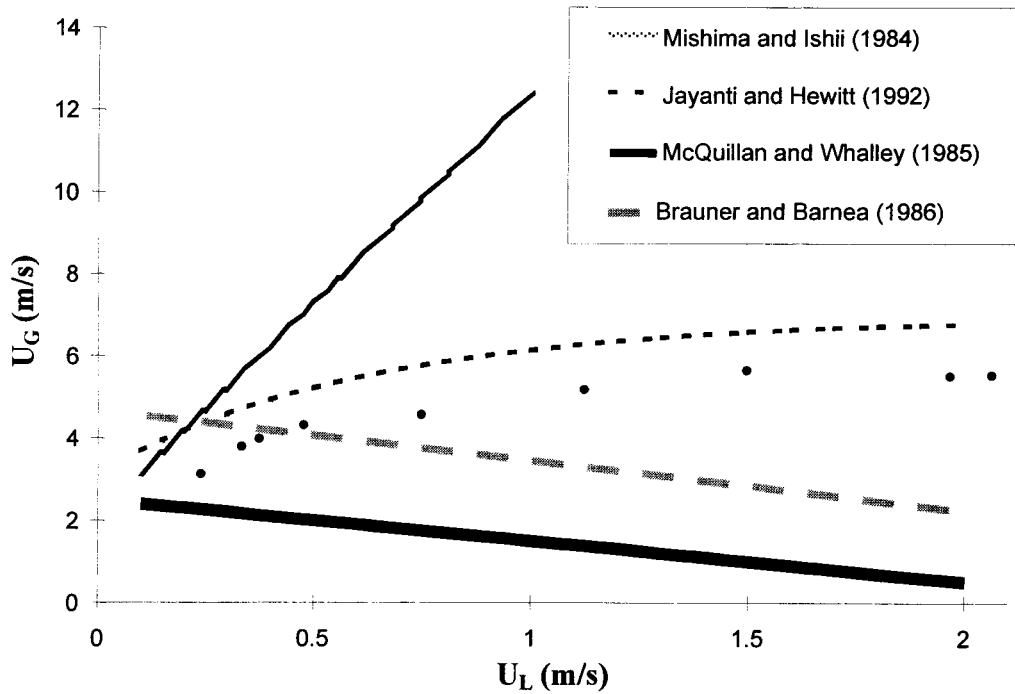


Fig. 13. A 1.2-bar result comparison.

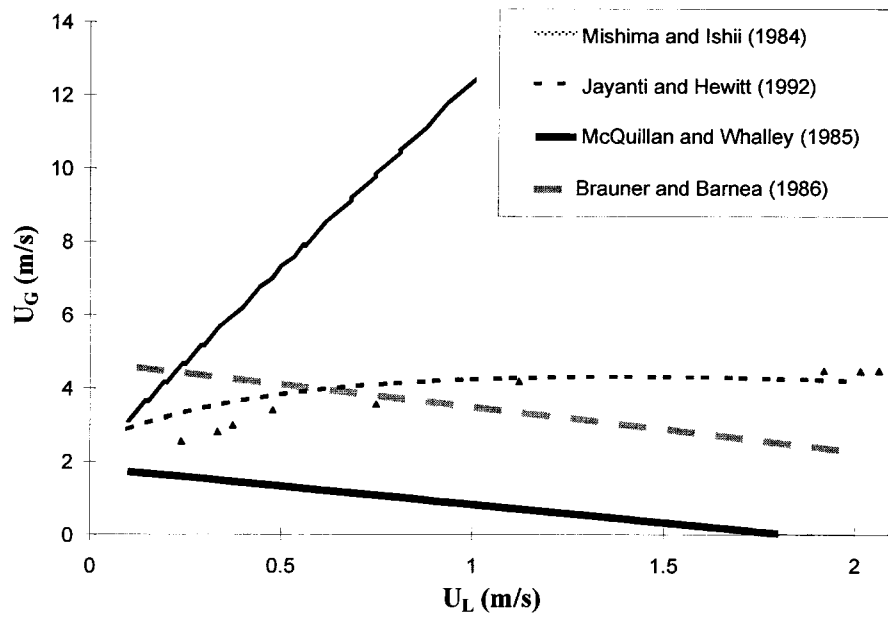


Fig. 14. A 3-bar result comparison.

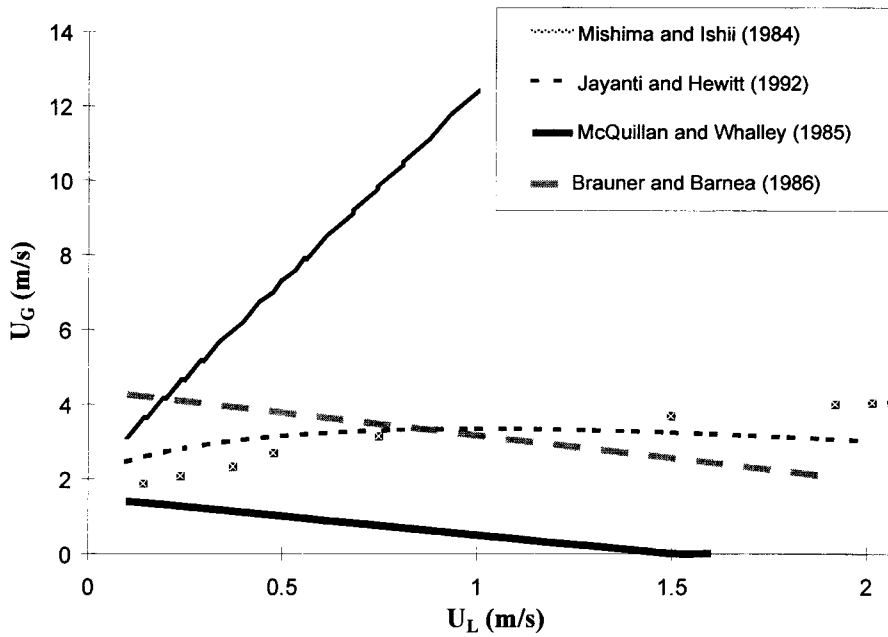


Fig. 15. A 5-bar result comparison.

increasing liquid superficial velocity, but predicts an increase in gas velocity with decreasing pressure as observed.

2. The model of Mishima and Ishii predicts that there is no effect of pressure (gas density) on the transition, contrary to the observations.
3. The model of Brauner and Barnea (1986) predicts that the mixture superficial velocity U_m is constant (for given fluid physical properties and tube diameter). Thus the transitions may be represented by a straight line of the form $U_G = U_m - U_L$. The predicted value of U_m for the present experiment at 1.2 bar is 4.528 ms^{-1} and the value at 6 bar is predicted to be 4.515 ms^{-1} . Thus, the predicted change with pressure is negligible (around 0.3%) whereas, the data show a systematic change with pressure of the order of 30% over the range covered. Moreover, the trend of variations of U_G with U_L for the transition is incorrectly predicted by the Brauner and Barnea model.
4. The model of Jayanti and Hewitt predicts the correct trends with both pressure and liquid velocity and is also in reasonable quantitative agreement with the data.

It would seem, therefore, that the Jayanti and Hewitt (1992) model gives the best predictions. Both this model and that of McQuillan and Whalley (1985) are based on the flooding hypothesis; the crucial difference between them is that the Jayanti and Hewitt model takes into account the film length, which is clearly necessary to predict the transition.

However, the Jayanti and Hewitt model over-predicts the effect of pressure as is shown in Fig. 16. The predictions are of the order 20% higher than the data at 1.2-bar pressure and are lower than the data at 5 bar, and higher liquid velocities.

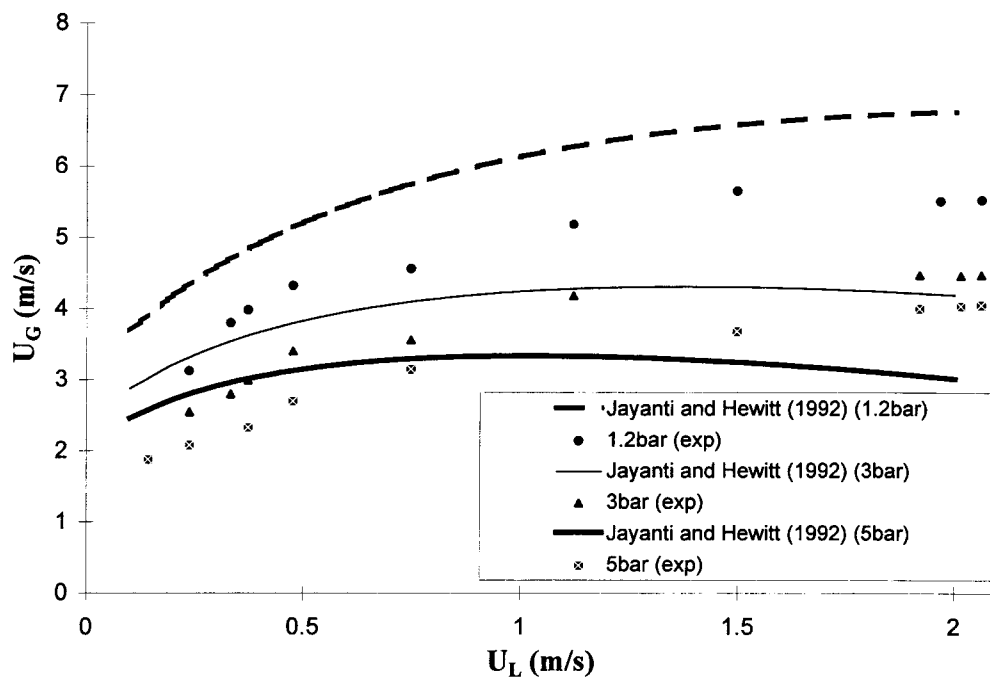


Fig. 16. Jayanti and Hewitt model compared to data.

5. Conclusions

The following conclusions can be drawn:

1. Experiments were carried using the impedance probability scheme developed by Costigan and Whalley (1997) to determine the slug to churn transition at various flowrates and pressures.
2. Over the limited range where the two could be compared, the results were in reasonable agreement with those of Costigan and Whalley (1997). However, the present data greatly extend the range of fluid velocities and pressures covered.
3. Increasing the liquid flowrate increases the gas flowrate required to initiate the slug/churn transition, though the effect is small at the highest range of liquid flowrates covered.
4. An increase in pressure decreases the superficial gas velocity at the transition.
5. The results were compared with the Mishima and Ishii (1984) and Brauner and Barnea (1986) (based on a critical void fraction in the slug). These models predicted that there was no or negligible effect of pressure on the transition, contrary to the observations. Of the two critical void fraction models, the Brauner and Barnea model was closest to the experimental data but (in addition to not predicting a significant effect of pressure) predicted the incorrect trend of the variation of U_G with U_L for the transition.
6. The flooding-type slug/churn models of McQuillan and Whalley (1985) and Jayanti and Hewitt (1992) both predict an effect of pressure but the McQuillan and Whalley model predicts the wrong trend with liquid velocity.
7. Overall, the model of Jayanti and Hewitt (1992) performed best in predicting the present data. The effect of pressure was, however, somewhat over-predicted by this model.

References

- Brauner, N., Barnea, D., 1986. Slug/churn transition in upward gas–liquid flow. *Chem. Eng. Sci.* 41, 159–163.
- Costigan, G., 1997. Flow pattern transitions in vertical gas–liquid flows. D.Phil. thesis, Oxford University.
- Costigan, G., Whalley, P.B., 1997. Slug flow regime identification from dynamic void fraction measurements in vertical air–water flows. *Int. J. Multiphase Flow* 23, 263–282.
- Jayanti, S., Hewitt, G.F., 1992. Prediction of the slug-to-churn flow transition in vertical two-phase flow. *Int. J. Multiphase Flow* 18, 847–860.
- Ma, Y.P., Chung, N.M., Pei, B.S., Lin, W.K., 1991. Two simplified methods to determine void fractions for two-phase flow. *Nucl. Technol.* 94, 124–133.
- McQuillan, K.W., Whalley, P.B., 1985. Flow patterns in vertical two-phase flow. *Int. J. Multiphase Flow* 11, 161–175.
- Mishima, K., Ishii, M., 1984. Flow regime transition criteria for upward two-phase flow in vertical tubes. *Int. J. Heat and Mass Transfer* 27, 723–737.
- Nicklin, D.J., Davidson, J.F., 1962. The onset of instability in two-phase flow systems. *Int. J. Multiphase Flow* 7, 311–320.
- Taitel, Y., Barnea, D., Dukler, A.E., 1980. Modelling flow pattern transitions for steady upward gas–liquid flow in vertical tubes. *AIChE J.* 26, 345–354.
- Wallis, G.B., 1969. *One-dimensional two-phase flow*. McGraw Hill, New York.

- Wang, Y.W., Pei, B.S., Lin, W.K., 1991. Verification of using a single void fraction sensor to identify two-phase flow patterns. *Nucl. Technol.* 95, 87–94.
- Watson, M.J., 1999. Flow pattern transitions and associated phenomena. PhD thesis, Imperial College, University of London.